Research Article

Unsteady Mhd Williamson And Casson Nano Fluid Flow In The Presence Of Radiation And Viscous Dissipation

P.Mangathai[1], B.Rami Reddy[2]challagundla Sidhartha[3]
[1]department Of Mathematics, Anurag Group Of Institutions, Ghatakesar, Ranga Reddy, India-500088.
[2]department Of Mathematics, Hindu College, Guntur, India-522002.
Email: Mangathai123@Gmail.Com

Article History: Received: 10 January 2021; Revised: 12 February 2021; Accepted: 27 March 2021; Published online: 4 June 2021

Abstract
The Mhd Laminar Boundary Flow With Heat And Mass Transfer An Electrically Leading Mhd Williamson And Casson Nano Fluid Over A Penetrable Extending Sheet Installed In A Permeable Medium Has Been Considered In The Impacts Of Attractive Field, Thermal Radiation, And Compound Response. The Administering Halfway Differential Conditions Alongside The Boundary Conditions Were Diminished To Dimensionless Structures By Utilizing Reasonable Closeness Change. The Subsequent Arrangement Of Common Differential Conditions With The Relating Boundary Conditions Was Illuminated Through Runge-Kutta Fehlberg Strategy Alongside Shooting Method. The Consequences Of The Investigation Show That Velocity, Temperature, And Concentration Boundary Layer Thicknesses By And Large Diminishing As We Move Away From The Outside Of The Extending Sheet And The Williamson And Casson Parameter Was Found To Impede The Velocity Profiles. The Physical Parameters Like Skin Friction, Nusselt Number And Sherwood Number Are Discussed In Detail.

Keywords: Radiation, Casson Fluid, Mhd, Heat And Mass Transfer, Skin-Friction.

1.0 Introduction

The Model Of Heat Along With Mass Transport Of Non-Newtonian Fluids Past A Permeable Stretching Sheet In A Loopholes Medium Is Of Interest To Many Engineers And Scientist In Recent Years. Their Interest Arose Because Of Its Usefulness In Pipe Industry, Annealing, Food Processing, Extrusion Process Etc. The Non-Newtonian Fluids Portray Shear Stress Variation Along With Some Fluid Physical Properties. Hence, It Is Categorized As Viscoelastic, Cross Model, Dilatant, Bingham Plastic, Pseudoplastic, Casson Model Etc. Many Engineers And Scientist Have Found This Type Of Non-Newtonian Models Very Difficult To Solve Because Of Their Complexity And Nonlinearity Of Their Model Equations. The Nonlinearity Of This Type Of Fluid Is Evident In Drilling Operations And Bioengineering. To Overcome These Challenges, Rheological Equations Of Different Types Have Been Adopted On Each Model And Numerical Approach Has Been Used By Past Researchers To Profound Solutions. Mahmoud And Waheed [1] Elucidate Mhd Flow Along With Heat Transport Of A Rotating Fluid. Their Model Equations Were Answered By Employing Chebyshev Spectral Method. Nadeem Et Al. [2] Explored Transport Of Williamson Fluid In A Stretching Sheet. They Solved Their Flow Model Using Homotopy Analysis Approach And Concluded That Velocity Degenerate With Increasing Value Of Williamson Parameter. Bilal Et Al. [3] Studied Thermally Stratified Williamson Fluid Transport Using Numerical Approach. They Concluded That Williamson Parameter Degenerate Velocity Profile. Eldabe And Abou-Zeid [4] Examined Mhd Pulsatile Flow Of Non-Newtonian Nanofluid Along With Heat Transport. They Discovered That Chemical Reaction Parameter Degenerate The Nanoparticles Phenomena. Bilal Et Al. [5] Elucidate Mhd Along With Thermal Radiation On Williamson Nanofluid Flow Numerically. They Discovered That Velocity Profile Degenerate Because Of Increase In Weissenberg Number. Khan Et Al. [6] Elucidate Impact Of Heat Along With Mass Transport On Williamson Nanofluid Flow. Their Flow Model Was Solved Numerically And They Discovered That Wall Friction Factor Degenerate For Large Values Of Weissenberg Number. Idowu And Falodun [7] Explored Mhd Heat Along With Mass Transport Of Walters-B Viscoelastic Fluid Employing Numerical Approach. They Discovered That Velocity Profile Degenerate Close To The Plate Because Of Increase In Viscoelastic Parameter. Lund Et Al. [8] Explored Movement Of Mhd Williamson Fluid Alongside Slippage. They Solved Their Flow Model Using Runge-Kutta. Heat Along With Mass Transport Phenomena Of Nanoparticles Of Williamson Fluid Situated In Heated Surface Have Been Elucidated By Hashim Et Al. [9]. They Discovered That Increasing The Unsteadiness Parameter Degenerate The Fluid Flow Fields. Transport Of Williamson

Fluid Because Of Nonlinearly Stretching Sheet Has Been Elucidated By Megahed [10]. Their Flow Model Was Answered By Employing Shooting Method And They Observed That Increase In Williamson Parameter Lead To Enhancement Of Temperature Distribution. Naganthran Et Al. [11] Considered Dilatants Nanofluid Effects Conveying Microorganism By Employing Scaling Group Analysis.

Studies On Non-Newtonian Casson Fluid On Heat Along With Mass Transport Alongside Nanoparticles Are Getting More Interest In The Specialization Of Applied Mathematics Because Of Its Wide Applications In Engineering. The Biological Fluids Of These Type Are Blood, Salvia Etc While Foodstuffs Are Jellies, Jams, Soups Etc. These Fluids Are Non-Newtonian Because They Never Obey The Linearity Nature Of Newtonian Fluid. Hence, Study On Casson Nanofluid Finds Applications In Biological Science, Biomedical, Bioengineering As Well As Industrial Engineering Where Food Is Processed. Reddy [12] Elucidate Mhd Transport Of Cason Fluid In Exponentially Inclined Permeable Stretching Surface. Their Transport Model Was Numerically Solved Using Shooting Method And They Discovered That Thickness Of Momentum Boundary Layer Degenerate Because Of Large Casson Parameter. Ullah Et Al. [13] Examined Hydrodynamic Falkner-Skan Transport Of Casson Fluid Using Keller Box Method. They Concluded That Raising Casson Parameter Enhances The Fluid Fields. Ghadikolaei Et Al. [14] Investigated Impact Of Nonlinear Thermal Radiation On Magneto Casson Nanofluid Transportation Alongside Joule Heating. They Concluded That Velocity Profile Degenerate With Increasing Effect Of Casson Parameter Flow Using Numerical Approach. They Concluded That As Casson Parameter Approaches Infinity, They Obtained A Newtonian Model. Fagbade Et Al. [15] Considered Transport Of Walters-B Liquid Fluid Past An Accelerating Permeable Surface. Their Results Show Degeneration In Velocity Profile Because Of Increase In Viscoelastic Parameter. Falodun Et Al. [16] Elucidate Heat Along With Mass Transport Of Casson Fluid. They Employed Numerical Approach On Their Flow Model And Concluded That The Casson Parameter Has Great Impact On Velocity Flow Field. The Recent Study Of Idowu And Falodun [17] Was On Heat Along With Mass Transport Of Mhd Casson Nanofluid. Their Flow Model Was Solved Numerically And They Concluded That Casson Parameter Behaves Like Newtonian As Its Value Approaches Infinity. Vijaya And Reddy [18] Elucidate Mhd Non-Darcy Flow Of A Casson Fluid By Considering Critical Parameters Of Thermophorosis.

The Studies Of Nanofluids Have Contributed Significantly To Research In Pharmaceutical Materials. Nanoparticles Is Very Useful In Delivering Of Drugs. It Is Also Useful In Treating Water As Well As Brain Tumors. Drugs Through The Help Of Nanoparticles Reach The Desired Organ With The Help Of Diffusion. Due To This Fact, The Side Effect Of Drugs Used By Animals Can Be Effectively Controlled. The Nanofluid Contains Nanometer-Sized Particles. Its Study Can Be Homogeneous Or Two-Phase Methods. The Nanofluid Has Large Colloidal Suspension Stability Together With Its Significance In Heat Transport. Kalteh [19] Examined Nanoparticle Along With Base Fluid On Heat Together With Fluid Flow Of Nanofluids. They Solved Their Flow Model Numerically And Discovered That Heat Transport Coefficient Is Higher That Water-Based Nanofluids. Ahmed And Nadeem [20] Elucidate Shape Impact Of Cu-Nanoparticles In Unsteady Flow. They Employed Perturbation Analytical Approach And They Concluded That Balloon Height Enhances Shear Stresses Along With Velocity Gradient. Farooq Et Al. [21] Elucidate Melting Heat Transport Along With Double-Stratification In Viscous Nanofluid Stagnation Flow. They Concluded That Fluid Temperature Improves Due To Increase In Thermophoretic Parameter. Bowers Et Al. [22] Elucidate Flow Together With Heat Transport Behavior Of Nanofluids Situated In Micro Channels. They Concluded That Their Tested Nanofluids Lead To Enhanced Heat Transport Properties. Khan And Alqahtani [23] Explored Mhd Nanofluids In A Penetrable Channel Along With Porosity. Chamkha Et Al. [24] Explored Similarity Solution For Unsteady Heat Along With Mass Transport. Mukhopadyay And Gorla [25] Examined Unsteady Mhd Boundary Layer Flow Of An Upper Convected Maxwell Fluid. In The Study Of Khan And Azam [26], Unsteady Heat Along With Mass Transport Mechanisms In Mhd Carreau Nanofluid Flow Was Examined. The Recent Work Of Tesfaye Et Al. [27] Considered Heat Together With Mass Transport In Unsteady Boundary Layer Flow Of Williamson Nanofluids. Santoshi Et Al. [28] Recently Examined 3d Casson Carreau Nanofluid Flow Using Numerical Approach.

In All The Previous Studies Discussed Above, None Of The Study Considered Heat Along With Mass Transport Of Casson And Williamson Nano Fluid Simultaneously. Studies On Nano Fluid Is Either Casson Or Williamson But Not Elucidated Together. Hence, The Present Exploration Is Aimed At Elucidating Heat Along With Mass Transport Of An Electrically Conducting Mhd Boundary Layer Flow Of Casson And Williamson Nano Fluid Over A Penetrable Stretching Sheet Situated In Porous Medium. Model Of This Type Has Not Been Considered In Literature To The Very Best Of Our Knowledge. We Have Embarked On This Study Because Of Its Applications In Biological Sciences, Biomedical, Bioengineering As Well As Food Processing. The Behavior Of The Two Non-Newtonian Fluids Is Examined By Plotting Graphs For Different Flow Parameters. Also, We Presented In Tabular Form The Physical Quantities Of Engineering Interest.

2.0 Mathematical Formulation

Unsteady Incompressible, Chemically Reacting And Thermally Transmitting Non-Newtonian Mhd Williamson And Casson Nano Fluidflow Over A Warmed Penetrable Extending Sheet Implanted In A Permeable Medium Were Thought Of. The Cartesian Arrange Structure Has Been Used With The End Goal That The X-Axis Is Along The Broadening Sheet, Y-Axis Is Typical To The Sheet, The Start Is Arranged At The Cut, And The Stream In The Region Y≥0. Presently, Tolerating That The Sheet Starts Reaching Out At T=0 And Expands On A Level Plane With Non-Uniform Velocity $U_w = ax/(1-ct)$, Where And Are Genuine Positive Constants. It Was Normal That The Alluring Reynolds Number Is Little In Liquid Metals And Fairly Ionized Fluids And The Effect Of Polarization Of Charges Isn't Thought Of. Along These Lines, The Started Alluring Field Is Insignificant In Relationship With The Applied Appealing Field. It Was Furthermore Expected That The Stream Is Created From A Cut By Stretching Out Of A Reliably Vulnerable And Semi-Unlimited Level Plate With One End Fixed At The Cut And Introduced In An Optically Thick Porous Medium.

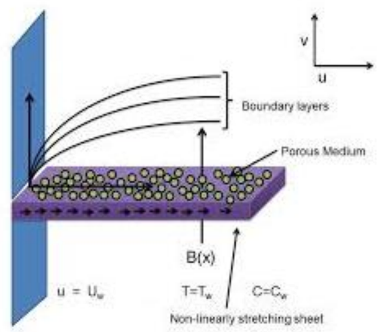

Fig. Physical Model Of The Problem

The Constructive Equation For The Casson Fluid Can Be Written As:

$$\tau_{ij} = \begin{cases} 2\left(\mu_B + \dfrac{P_y}{\sqrt{2\pi}}\right)e_{ij}, \pi > \pi_c \\ 2\left(\mu_B + \dfrac{P_y}{\sqrt{2\pi_c}}\right)e_{ij}, \pi < \pi_c \end{cases} \tag{1}$$

Where τ_{ij} Is The $(i,j)^{th}$ Stress Tensor Component. μ_B Is The Synthetic Dynamic Viscosity Of The Non-Newtonian Fluid, p_y Is The Yield Stress Of The Fluid, π Is The Product Of The Component Of Deformation Rate With Itself, Namely, $\pi = e_{ij}e_{ij}$, And e_{ij} Is The $(i,j)^{th}$ Component Of Deformation Rate, And π_c Is Critical Value Of Π Based On Non-Newtonian Model.

Under The Above Suspicions, The Limit Layer Conditions By The Boussinesq's Estimation, The Progression Condition, The Velocity Force, Temperature And Species Concentration Are Portrayed As Follows:

$$\frac{\partial u}{\partial x} + \frac{\partial v}{\partial y} = 0 \tag{2}$$

$$\frac{\partial u}{\partial t}+u\frac{\partial u}{\partial x}+v\frac{\partial u}{\partial y}=\nu\left(1+\frac{1}{\beta}\right)\frac{\partial^2 u}{\partial y^2}-\left[\frac{\sigma B_0^2}{\rho_f\left(1-ct\right)}+\frac{\nu}{K}\right]u+\sqrt{2}\nu\Gamma\frac{\partial u}{\partial y}\frac{\partial^2 u}{\partial y^2} \tag{3}$$

$$\frac{\partial T}{\partial t}+u\frac{\partial T}{\partial x}+v\frac{\partial T}{\partial y}=\alpha\frac{\partial^2 T}{\partial y^2}+\tau\left(D_B\frac{\partial C}{\partial y}\frac{\partial T}{\partial y}+\frac{D_T}{T_\infty}\left(\frac{\partial T}{\partial y}\right)^2\right)-\frac{1}{\rho Cp}\frac{\partial q_r}{\partial y} \tag{4}$$

$$\frac{\partial C}{\partial t}+u\frac{\partial C}{\partial x}+v\frac{\partial C}{\partial y}=D_B\frac{\partial^2 C}{\partial y^2}+\frac{D_T}{T_\infty}\frac{\partial^2 T}{\partial y^2}-Kr\left(C-C_\infty\right) \tag{5}$$

Where In The Directions x and y, The Velocity Constituents Are u and v, Individually, β Is The Casson Fluid Parameter, G Is The Gravitational Acceleration, ρ Is The Density Of The Fluids,ν Is The Kinematic Viscosity Of The Fluid, σ Is The Electrical Conductivity, α Is The Thermal Diffusivity, σ^* Is The Stefan-Boltzmann Constant, Cp Is The Specific Heat Constant Pressure,τ Is The Ratio Of Effective Heat Capacities Of Nanoparticles, T Is The Temperature Of The Fluid, C Is The Concentration Of The Fluid, D_b Is The Brownian Diffusion Coefficient, D_t Is The Thermophoresis Diffusion Coefficient And Kr Is The Chemical Reaction Parameter.

The Boundary Conditions For The Velocity, Temperature And Concentration Are Defined As

$$\text{At } y=0,\begin{cases} u=U_w\left(x,t\right)=\dfrac{ax}{1-ct}, v=V_w\left(t\right)=-\dfrac{V_0}{\sqrt{1-ct}}, \\ T=T_w\left(x,t\right)=T_\infty+\dfrac{T_0U_wx}{\nu\sqrt{1-ct}}, C=C_w\left(x,t\right)=C_\infty+\dfrac{C_0U_wx}{\nu\sqrt{1-ct}} \end{cases} \tag{6}$$

and as $y\to\infty$ $u\to 0, T\to T_\infty, C\to C_\infty$,

For An Optically Thick Fluid, The Vitality Condition (4) Can Likewise Be Decreased By Applying Rosseland Dispersion Guess For The Radiative Heat Flux Given By

$$q_r=-\frac{4\sigma^*}{3k^*}\frac{\partial T^4}{\partial y} \tag{7}$$

Where K* Is The Mean Ingestion Coefficient And σ^* Is Stefan-Boltzmann Consistent. In The Event That The Temperature Contrast Inside The Stream Is Extremely Little, At That Point It Tends To Be Extended T^4 In Taylor Arrangement About T_∞, Which Subsequent To Ignoring Higher Request Terms Takes The Structure

$$T^4=4T_\infty^3T-3T_\infty^4 \tag{8}$$

So That The Heat Flux Can Be Approximated As

$$q_r=-\frac{16T_\infty^3\sigma^*}{3k^*}\frac{\partial T}{\partial y} \tag{9}$$

Using Equations (9), The Energy Equation (4) Can Be Written As

$$\frac{\partial T}{\partial t}+u\frac{\partial T}{\partial x}+v\frac{\partial T}{\partial y}=\alpha\frac{\partial^2 T}{\partial y^2}+\tau\left(D_B\frac{\partial C}{\partial y}\frac{\partial T}{\partial y}+\frac{D_T}{T_\infty}\left(\frac{\partial T}{\partial y}\right)^2\right)+\frac{16\sigma^*}{3\rho Cpk^*}\frac{\partial^2 T}{\partial y^2} \tag{10}$$

In Order To Simplify The Mathematical Analysis, The Following Similarity Transformation Was Introduced:

$$\eta=y\sqrt{\frac{U_w}{\nu x}}, \xi\left(x,y,t\right)=\sqrt{U_w\nu x}\,f\left(\eta\right), \frac{T-T_\infty}{T_w-T_\infty}=\theta\left(\eta\right), \frac{C-C_\infty}{C_w-C_\infty}=\phi\left(\eta\right), \tag{11}$$

Using The Relations (11), The Boundary Layer Governing Equations (3),(5) And (6) Can Be Written In A Non-Dimensional Form Of The System Of Nonlinear Ordinary Differential Equations:

$$\left(1+Wef''\right)\left(1+\beta^{-1}\right)f''' + ff'' - A\left(0.5\eta f'' + f'\right) - f'^{2} - \left(M + K^{-1}\right)f' = 0 \tag{7}$$

$$\left(1+\frac{4}{3}R\right)\theta'' + \Pr\left[\left(f\theta' - 2f'\theta\right) - 0.5A\left(\eta\theta' + 3\theta\right) + Nb\theta'\phi' + Nt\left(\theta'\right)^{2}\right] = 0 \tag{8}$$

$$\phi'' + Sc\left[f\phi' - 2f'\phi - 0.5A\left(\eta\phi' + 3\phi\right)\right] - KrSc\phi + \frac{Nt}{Nb}\theta'' = 0 \tag{9}$$

Subject To The Corresponding Boundary Conditions Are:

$$\begin{aligned} &f = S,\ \ f' = 1,\ \ \theta = 1,\ \ \phi = 1 \quad \text{at} \quad \eta = 0 \\ &f' \to 0,\ \ \theta \to 0, \phi \to \infty \quad \text{as} \quad \eta \to \infty \end{aligned} \tag{10}$$

The Skin-Friction, Nusselt Number And Sherwood Number Are Important Physical Parameters For This Type Of Boundary Layer Flow.

The Skin Friction Coefficient C_f Is Defined As

$C_f = \dfrac{\tau_w}{0.5U_w^2}$, Where τ_w Is The Shear Stress At The Permeable Surface.

The Local Nusselt Number Is A Dimensionless Heat Transfer Coefficient Defined As Follows:

$$Nu = -\left(1+\frac{4}{3}R\right)\mathrm{Re}_x^{0.5}\,\theta'(0).$$

The Local Sherwood Number Is A Dimensionless Mass Transfer Coefficient Defined As Follows:

$$Sh = -\mathrm{Re}_x^{0.5}\,\phi'(0).$$

Where $\mathrm{Re}_x = \dfrac{ax^2}{\nu(1-ct)}$ Is The Local Reynolds Number.

3.0 Methodology

The Converted Nonlinear Differential Equations (7)–(9) With The Boundary Conditions (10) Are Elucidated By Runge-Kutta Fehlberg Method Along With Shooting Technique. This Method Has Been Proven To Be Adequate And Gives Accurate Results For The Boundary Layer Equations:

4.0 Results And Discussion

The Model Of Heat Along With Mass Transport, Laminar, Viscous Boundary Layer Flow Of An Electrically Conducting Mhd Williamson Together With Casson Nanofluid Over A Permeable Stretching Sheet Situated In A Porous Medium Has Been Elucidated In This Study. The Flow Model Equations Resulted To Nonlinear Partial Differential Equations Which Were Simplified Using Similarity Transformation. The Transformed Flow Equations (7)-(9) Along With (10) And (11) Have Been Solved Numerically By Adopting Runge-Kutta Fehlberg Method Together With Shooting Techniques. In Other To Explain The Physics Of The Present Problem, Flow Parameters Are Displayed Using Diagrams. The Present Exploration Is Of Great Interest In Engineering And We Hereby Caluculate Numerical Values Of Different Flow Parameters For Local Skin Friction, Sherwood As Well As Nusselt Number Are Presented In Tabular Form. During Our Numerical Experiments, We Set $M = 0.5, K = 1.0, We = 0.2, \beta = 0.3, Pr = 0.72, A = 0.3, Sc = 1.0, R = 0.2, Kr = 0.2, S = 0.3, Nb = 0.2, Nt = 0.1$. These Values Are Valid For All Graphs And Table Unless We State Another Value For A Specified Graph Or Table.

Figure 2(A) Portrays The Behavior Of Magnetic Parameter (M) On Velocity Profile. It Is Obvious From Figure 2(A) That Increases In M Leads To Degeneration Of Velocity Profile. Since We Imposed Transverse Magnetism On The Simultaneous Flow Of Williamson Along With Casson Nanofluid, A Drag-Like Force (Lorentz Force) Arises. The Responsibility Of This Force Is To Slow Down The Motion Of An Electrically Conducting Fluid. Hence, This Force Is Responsible For The Declination Of Velocity Profile As Shown In Figure 2(A). Our Experiment Shows That, The Velocity Profile As Shown In Figure 2(A) Diminishes Gradually From The Wall To The Dimensionless Distance$(i.e\ \ \eta \to \infty)$. Due To The Non-Uniform Velocity As Seen In The Momentum Equation (3), The Decrease In The Fluid Motion Is Not Uniform Starting From The Initial Point To The Boundary Which Tends To Zero. Physically, If The Product Of Electrically Conductivity (σ) And The Strength Of The Magnetic Force Is More Than The Fluid Density, Lorentz Force Posses More Electromagnetic Force Which Pull Down And Drag Back The Fluid Motion The More. Figure 2(B) Illustrates The Effect Of Permeability Parameter (K) On Velocity Profile. The Permeability Stretching Sheet Gives Way To Movement Of Casson Along With Williamson Nanofluid Within The Boundary Layers. Ideally, The Hole Allows Steady Flow Of Casson And Williamson Fluid Mixture Within The Boundary Layers. Their Transport Within The Layers Becomes Very High The Moment K Increases. This Is Evident In Figure 2(B) As Increase In K Leads To Enhancement Of Velocity Profile As Well As Thickness Of Momentum Boundary Layer.

The Effect Of Weissenberg Parameter (We) On Velocity Profile Is Illustrated In Figure 3(A). Increasing The Value Of We Is Noticed To Degenerate The Velocity Profile. As We Increases Over Stretchable Sheet, It Repels The Thickness Of The Layers To Degenerate The Velocity Profile. In Addition, The Decrease In Velocity Profile Because Of Increase In We Is Due To The Transversely Magnetic Field Imposed On The Flow. The Imposed Magnetism Drags The Flow Of Williamson Fluid And Thereby Degenerate The Fluid Velocity Along With Momentum Boundary Layer Thickness. Figure 3(B) Portrays The Impact Of Unsteadiness Parameter (A) On Velocity Profile. (A) Is Noticed To Degenerate The Velocity Profile As Its Value Increases. The Effect Of Casson Parameter (β) On Velocity Profile Is Depicted In Figure 4(A). Increasing The Value Of β Declines The Velocity Profile As Illustrated In Figure 4(A). Our Experiment Shows That, The Flow Of Casson Nanofluid In The Presence Of Lorentz Force Is Responsible For β To Degenerate The Fluid Motion. In Addition, The Yield Exhibiting Fluid Possesses A Plastic Dynamic Viscosity. Viscosity Gives Resistance To Fluid Flow. Hence, The Plastic Dynamic Viscosity Which Is Considered Constant In This Study Is Another Yardstick For Higher β To Decline The Fluid Velocity. This Means That An Amplified Plastic Dynamic Viscosity Produces Greater Resistance To The Flow. The Values Of β Is Chosen Between 0.1, 0.2, 0.3, And 0.4. This Values Are Chosen To Be Small Because We Observed That As We Keep Increasing The Value Of β $(i.e\ \ as\ \ \beta \longrightarrow \infty)$, The Present Model Transformed To Be Only Flow Of Williamson Nanofluid. This Means That When $\beta \longrightarrow \infty$ In The Viscosity Term $\nu\left(1+\frac{1}{\beta}\right)\frac{\partial^2 u}{\partial y^2}$ We Have $\nu\left(1+\frac{1}{\infty}\right)\frac{\partial^2 u}{\partial y^2} = \nu\frac{\partial^2 u}{\partial y^2}$. Obviously, The Casson Fluid Model Is Negligible As $\beta \to \infty$. Figure 4(B) Illustrates The Effect Of Suction Parameter On Velocity Profile. The Thicknesses Of The Momentum Boundary Layer Degenerate Due To Increase In Suction Velocity. This Means That The Mixture Of β And We Moves Closer To The Stretching Surface And Hereby Reduces The Fluid Velocity. Hence, The Presence Of Wall Suction Declines Velocity Boundary Layer Thickness.

Figure 5(A) Portrays The Effect Of Prandtl Number $(\Pr)$ On Temperature Profile. $\Pr = \frac{\rho c_p}{k^*}$ Is Noticed To Decrease The Temperature Profile. It Worth Noting That Thermal Diffusivity $\alpha = \frac{1}{\rho c_p}$, Hence $\Pr$ Is The Inverse Of Thermal Diffusivity. $\Pr$ Is Noticed To Degenerate The Temperature Profile Gradually From The Wall. This Is Because There Is No Much Viscosity Far Away From The Plate. Greater $\Pr$ Is Very Useful In Controlling Thermal Diffusivity As Well As Momentum Diffusivity In Heat Along With Mass Transport Problem. Note That $\Pr = 0.72, 1.0, 3.0, 7.0$ Used In This Study

Implies $\Pr$ For Water. Hence, When $\Pr << 1$ It Implies Thermal Diffusivity Controls The Flow Behavior While $\Pr >> 1$ Implies Momentum Diffusivity Controls The Flow Behavior. Therefore, $\Pr$ Is Useful In Controlling Cooling Rate Of An Electrically Conducting Fluid. In This Study, There Exist A Wall Temperature T_w And Free Stream Temperature T_∞ Which Gives Rise To $(T_w - T_\infty)$ Along With Thermal Boundary Layer Thickness. Figure 5(B) Portrays The Impact Of Unsteadiness Parameter (A) On Temperature Profile. Increasing The Value Of (A) Is Noticed To Degenerate The Temperature Profile. The Presence Of (A) Together With M And $\Pr$ Drags The Random Mixing Of Casson And Williamson Fluid Within The Boundary Layer. As A Result Of This, The Temperature Along With Thermal Boundary Layer Declines Simultaneously. Figure 6 Illustrate The Effect Of Thermal Radiation (R) On The Temperature Profile. Increasing The Value Of R Is Observed To Enhance The Temperature Profile. Experimentally, Thermal Radiation Added More Heat Energy To The Thermal Boundary Layer. This Gives An Avenue For More Temperature And Thereby Enhances Temperature Profile. The Temperature Profile As Shown In Figure 6 Brings Increase To The Thermal Boundary Layer Thickness. The Two Non-Newtonian Williamson And Casson Nanofluid Considered In This Study Becomes Warm Due To The Presence Of Thermal Radiation Parameter. Now, Increasing This Parameter R Increases Their Temperature And The Thermal Boundary Layer Becomes Very Thick. Hence, R Is Important In The Problem Of Heat Along With Mass Transport When $R \neq 0$.

Figure 7(A) Portrays The Impact Of Schmidt Number (Sc) On Concentration Profile. Sc Is Indirectly Proportional To Brownian Diffusion And Thereby Degenerate The Concentration Boundary Layer. The Value Of $Sc = 0.22$ And 0.3 Means Helium, $Sc = 0.60$ Means Oxygen, $Sc = 0.78$ Means Ammonia. The Maximum Value Of Sc Used In This Study Is 0.78 Which A Value Is For Ammonia. Our Experiment Shows That Increase In Sc Up To 1 (One) Result To Spontaneous Diffusion Of The Species At The Same Rate As Momentum In Both Williamson And Casson Nanofluid. For The Case Of $Sc < 1$, Diffusivity Of The Species Becomes Greater Than Diffusivity Of Momentum. Now, If $Sc = 0$ It Implies Absence Of Specie Concentration. Hence, The Present Model Becomes Heat Transport. As A Result Of The Mixture And Diffusion Of Casson Together With Williamson Nanofluid, Increase In The Value Of Sc Hereby Reduces The Fluid Concentration Profile. Figure 7(B) Illustrates The Impact Of Chemical Reaction (Kr) On Concentration Profile. Increasing The Value Of Kr Is Noticed To Decrease The Concentration Profile. Chemical Reaction Takes Place The Moment Casson And Williamson Nanofluid Are Mixed Together Within The Boundary Layer. The Mixture Of These Two Fluids In The Presence Of Thermal Radiation And Magnetic Parameter Result To A Destructive Reaction. As A Result Of This Destructive Reaction, The Concentration Profile As Shown In Figure 7(B) Decreases. Figure 8(A) Portrays The Impact Of Brownian Motion (Nb) On The Concentration Profile. The Brownian Motion Parameter Is Noticed To Degenerate The Concentration Profile. Two Things May Be Responsible For This; (I) The Plastic Dynamic Viscosity In Casson Nanofluid Along With The Pseudo Plastic Nature Of Williamson Nanofluid; And (Ii) The Imposed Magnetic Field To The Direction Of Flow. The Two Facts Bring Resistance To The Flow Of An Electrically Conducting Fluid. Figure 8(B) Illustrates The Impact Of Thermophoretic Parameter On Concentration Profile. Thermophoresis Defines The Migration Of Small Particles From Hot Region To Cold Region. Now, When The Nanoparticles Migrate In The Presence Of Thermal Radiation Parameter, It Add More Particles During This Process. However, More Increase In Thermophoretic Parameter Increases The Thermophoretic Force And Velocity To Elevate The Concentration Profile. Figure 9 Illustrate The Impact Of Unsteadiness Parameter (A) On Concentration Profile. This Effect Is Noticeable As It Degenerate The Concentration Profile. The Yield Exhibiting Nanofluid And Williamson Nanofluid Both Possesses Viscosity Is Responsible For The Reduction In The Concentration Profile.

Table 1 Shows The Effect Of All Flow Parameters On The Skin Friction, Nusselt And Sherwood Number Respectively. Fixing All Other Parameters Constant And Increasing M , A Significant Increase In Local Skin Friction, Nusselt And Sherwood Number Is Observed. This Means That The Imposed Magnetic Field Helps To Boast The Fluid Heat Along With Mass Transport Rate. In The Same Vein, Increase In Permeability Parameter Is Observed To Enhance Skin Friction, Nusselt And Sherwood Number. This Means That The Consideration Of Casson And Williamson In The Present Study Is Good In Boasting The Flow Of Heat Together With Mass Transport. In Table 1, $\Pr$ Is Observed Not To Have Effect On Local Skin Friction But Enhances Nusselt As Well As Sherwood Number. This Means That $\Pr$ Can Be Use In Controlling Rate Of Heat And Mass Transfer. The Unsteadiness Parameter Is Observed In Table 1 To Boast The Entire Boundary Layer Thickness By Increasing Local Skin Friction, Nusselt And Sherwood Number. In Table 1, Increase In The Suction Parameter Is Negligible On Local Skin Friction But Increases The Nusselt And Sherwood Number. Also, In Table 1 Impact Of R, Nb, Kr And Nt Is Noticed To Be Negligible On Local Skin Friction But Brings Increase To The Nusselt And Sherwood Number.

4.1velocity Profiles

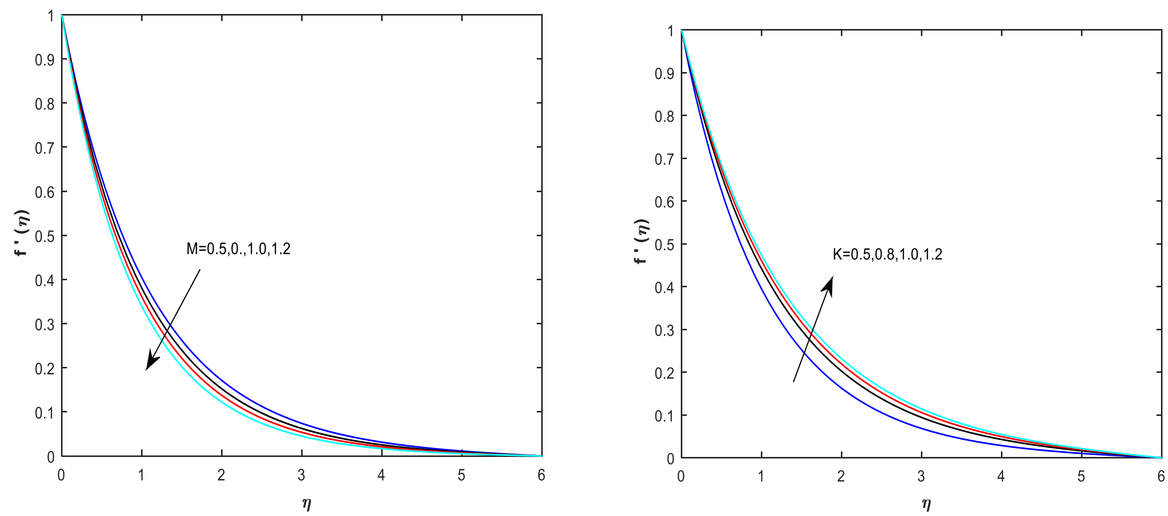

2(A) **2(B)**

Figure 2: Effect Of **2(A)** Magnetic Parameter (M); And **2(B)** Permeability Parameter On Velocity Profile

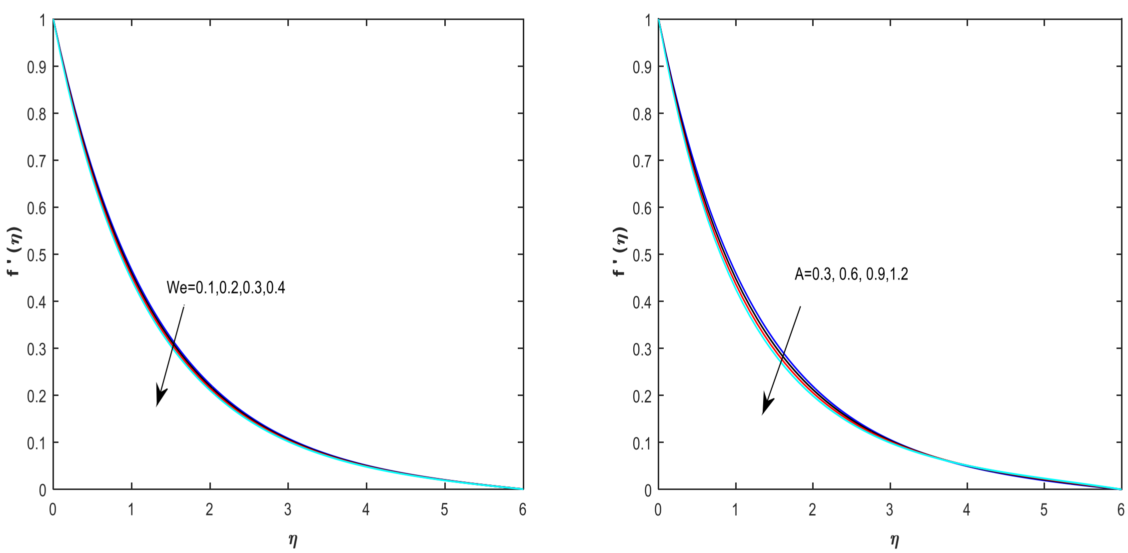

3(A) **3(B)**

Figure 3: Effect Of 3(A)Weissenber Parameter (We); And 3(B) Unsteadiness Parameter On Velocity Profile

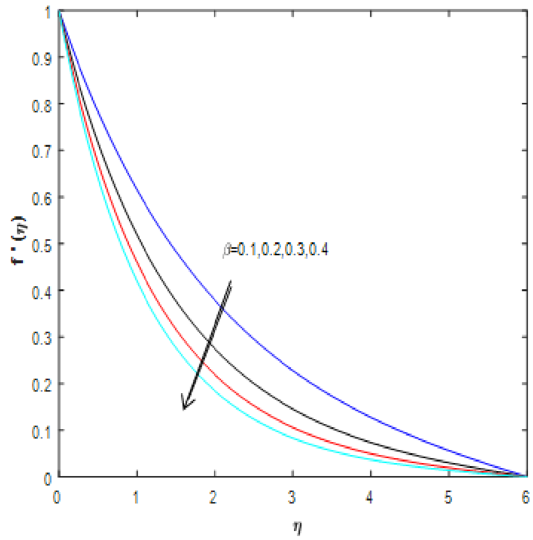

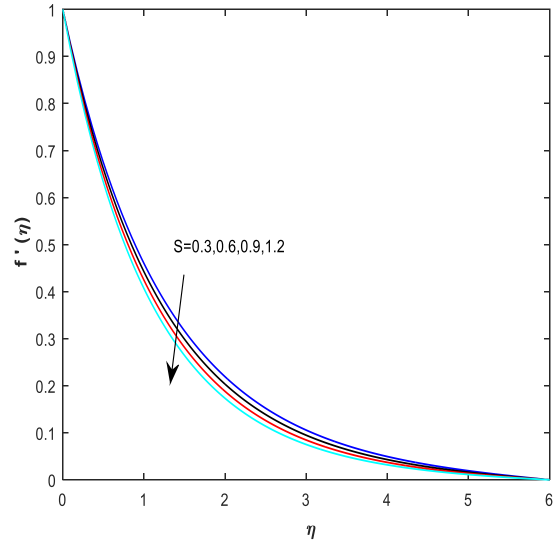

4(A) **4(B)**

Figure 4: Effect Of **4(A)** Casson Parameter(β); **4(B)** Suction Parameter On Velocity Profile

4.2 Temperature Profiles

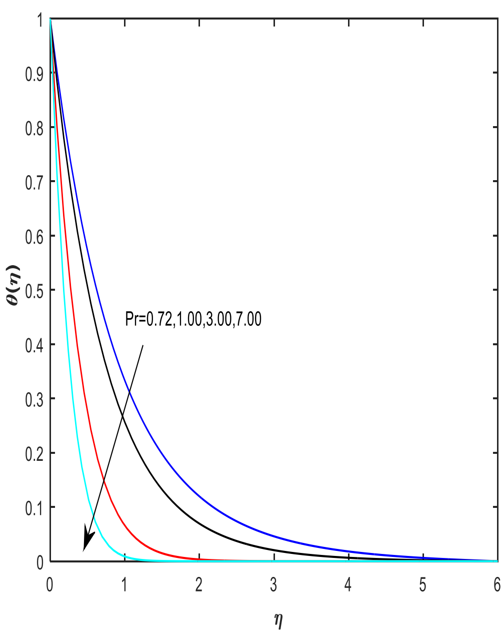

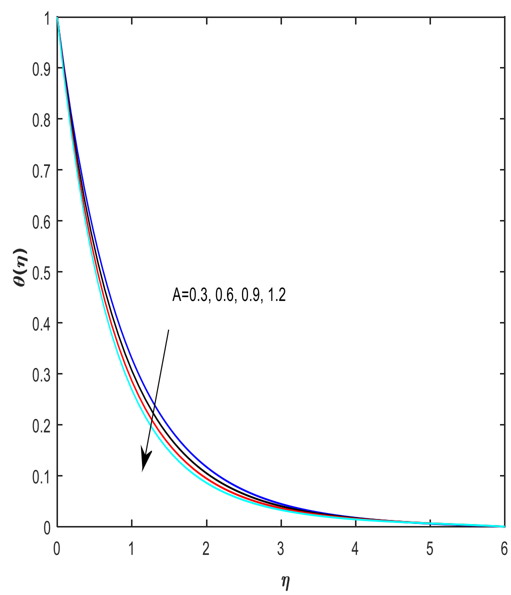

5(**A)** **5(B)**

Figure 5: Effect Of 5(A) Prandtl Number (Pr); And 5(B) Unsteadiness Parameter On Temperature Profile.

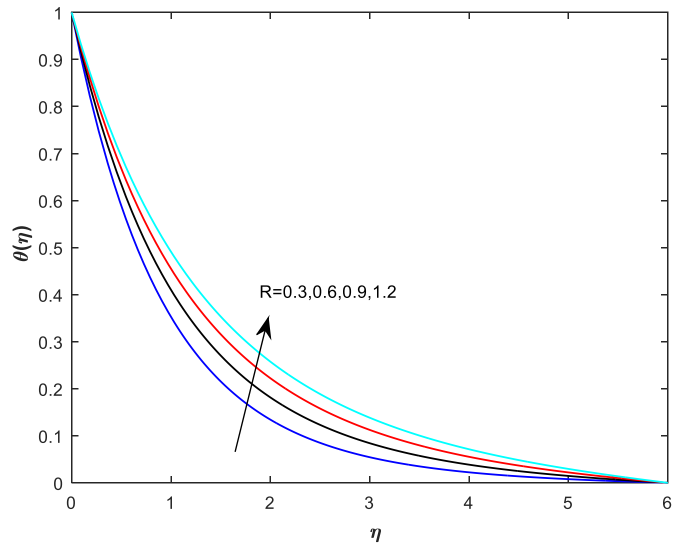

Figure 6: Effect Of Thermal Radiation Parameter (R) On Temperature Profile.

4.3 Concentration Profiles

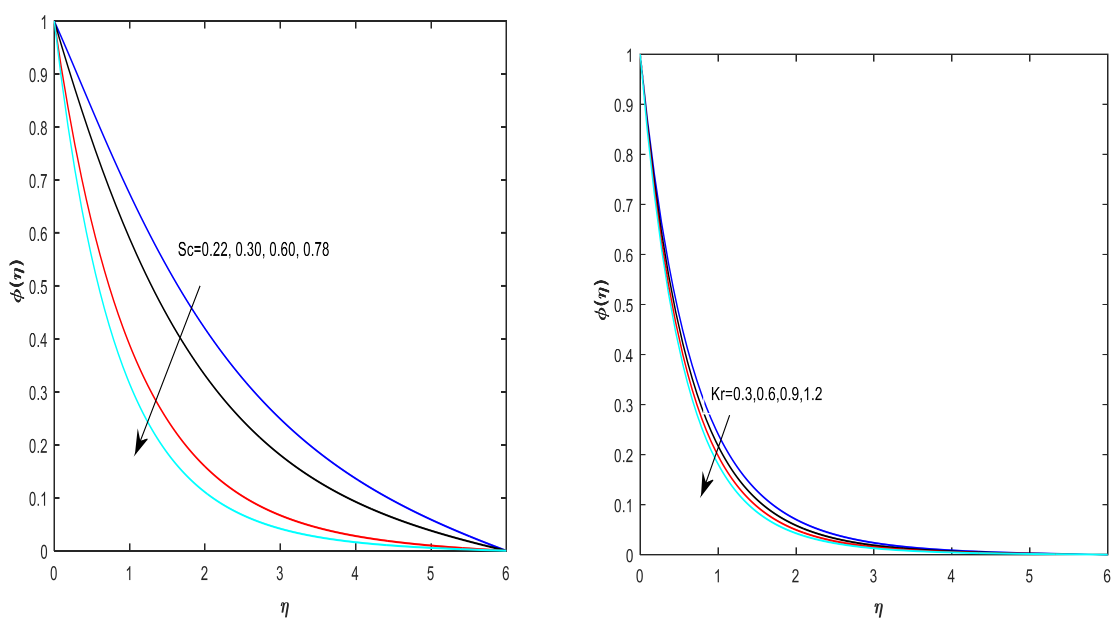

7(A) **7(B)**

Figure 7: Effect Of 7(A) Schmidt Number (Sc); And 7(B) Chemical Reaction Parameter On Concentration Profile.

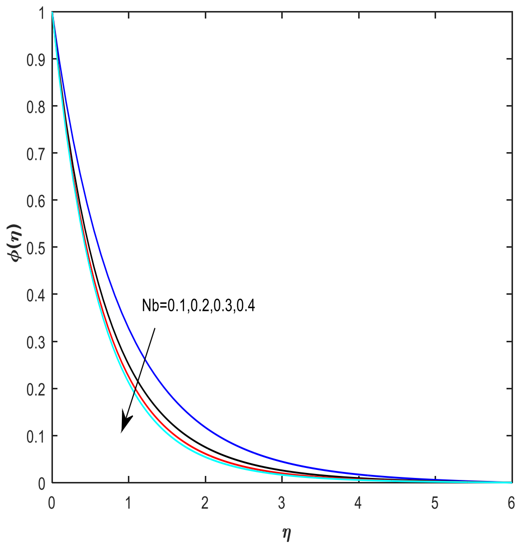

8(A)

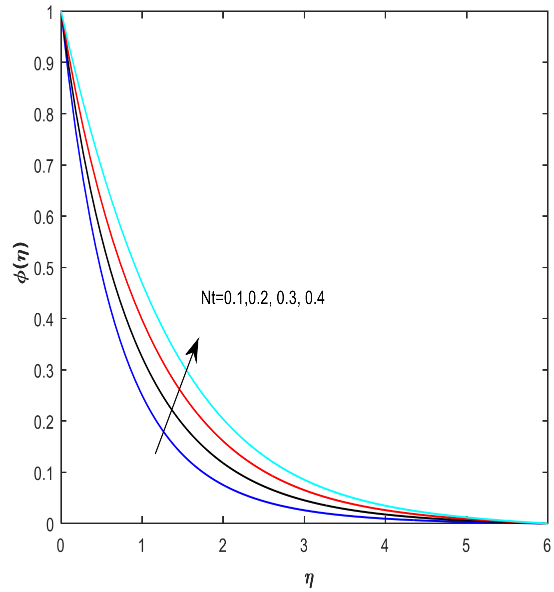

8(B)

Figure 8: Effect Of 8(A) Brownian Motion Parameter (Nb); And 8(B) Thermophoresis Parameter On Concentration Profile.

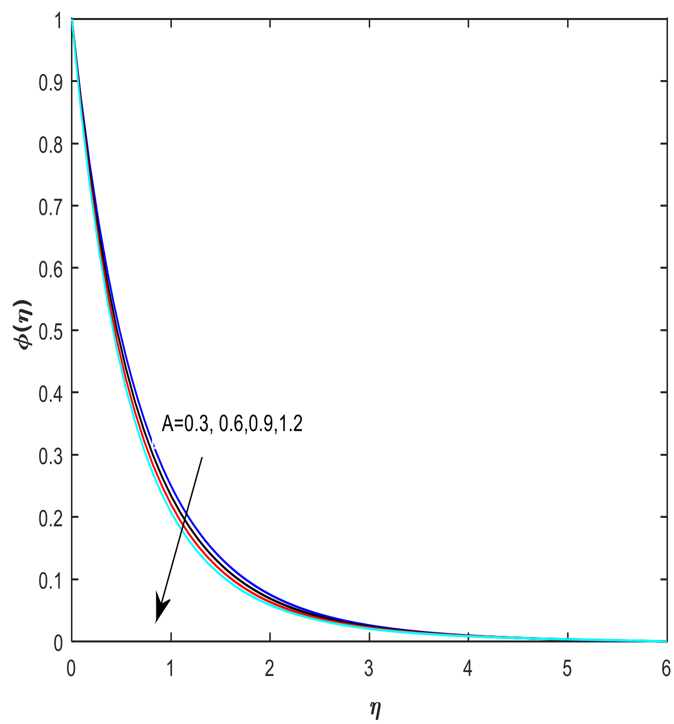

Figure 9: Effect Of Unsteadiness Parameter (A) On Concentration Profile.

Table 1: Numerical Computations Of Different Flow Parameters For Local Skin Friction, Nusselt And Sherwood Number.

M	**K**	**We**	$\boldsymbol{\beta}$	**Pr**	**A**	**Sc**	**R**	**Kr**	**S**	**Nb**	**Nt**	**Cf**	**Nu**	**Sh**
0.5	1	0.2	0.3	0.72	0.3	1	0.2	0.2	0.3	0.2	0.1	0.839432	1.096900	1.450930
0.8												0.904824	1.108132	1.462180
1												0.961976	1.118009	1.472082
1.2												1.028380	1.129528	1.483646
0.2	0.5	0.2	0.3	0.72	0.3	1	0.2	0.2	0.3	0.2	0.1	0.772072	1.107074	1.461121
	0.8											0.802447	1.128303	1.482415
	1											0.846327	1.136138	1.490290
	1.2											0.968160	1.141611	1.495799
0.2	1	0.1	0.3	0.72	0.3	1	0.2	0.2	0.3	0.2	0.1	0.778481	1.128733	1.482524
		0.2										0.802447	1.132667	1.486657
		0.3										0.830785	1.136138	1.490290
		0,4										0.865393	1.139251	1.493535
0.2	1	0.2	0.1	0.72	0.3	1	0.2	0.2	0.3	0.2	0.1	0.488943	1.118549	1.472566
			0.2									0.671490	1.136138	1.490290
			0.3									0.802447	1.159509	1.513919
			0.4									0.904394	1.193176	1.548189
0.2	1	0.2	0.3	0.72	0.3	1	0.2	0.2	0.3	0.2	0.1	0.802447	1.127301	0.470597
				1								0.802447	1.361499	0.994491
				3								0.802447	2.406985	1.410315
				7								0.802447	3.597694	1.493331
0.2	1	0.2	0.3	0.72	0.3	1	0.2	0.2	0.3	0.2	0.1	0.802447	1.136138	1.490290
					0.6							0.841285	1.225743	1.585572
					0.9							0.879210	1.308554	1.675491
					1.2							0.916227	1.385876	1.760743
0.2	1	0.2	0.3	0.72	0.3	0.22	0.2	0.2	0.3	0.2	0.1	0.802447	1.141720	0.316419
						0.3						0.802447	1.147551	0.485574
						0.6						0.802447	1.162080	0.985031
						0.78						0.802447	1.167879	1.227359
0.2	1	0.2	0.3	0.72	0.3	1	0.3	0.2	0.3	0.2	0.1	0.802447	0.753724	1.511444
							0.6					0.802447	0.830137	1.558675
							0.9					0.802447	0.931529	1.590905
							1.2					0.802447	1.074196	1.614425
0.2	1	0.2	0.3	0.72	0.3	1	0.3	0.3	0.3	0.2	0.1	0.802447	1.129685	1.528576
								0.6				0.802447	1.131336	1.636854
								0.9				0.802447	1.133200	1.737105
								1.2				0.802447	1.135344	1.830981
0.2	1	0.2	0.3	0.72	0.3	1	0.3	0.2	0.3	0.2	0.1	0.802447	1.136138	1.490290
									0.6			0.845284	1.222174	1.618917
									0.9			0.890581	1.314185	1.756176
									1.2			0.938400	1.411850	1.901452
0.2	1	0.2	0.3	0.72	0.3	1	0.3	0.2	0.3	0.3	0.1	0.802447	1.080202	1.184436
										0.6		0.802447	1.107816	1.490290
										0.9		0.802447	1.136138	1.592018

										1.2		0.802447	1.165181	1.642718
0.2	1	0.2	0.3	0.72	0.3	1	0.3	0.2	0.3	0.3	0.3	0.802447	1.090853	0.710012
											0.6	0.802447	1.105571	0.959565
											0.9	0.802447	1.120663	1.219497
											1.2	0.802447	1.136138	1.490290

Table 2: Comparison Of Results On $-f''(0)$ for $We = M = K = R = Sc = S = Kr = \beta = 0$, $\Pr = 0.72, N_b = 0.2, N_t = 0.1$ Against The Values Of Unsteadiness Parameter A.

A	Chamkha Et Al. [24]	Mukhopadyay And Gorla [25]	Khan And Azam [26]	Tesfaye Etal.[27]	Present Study
0.0	-----	---	1.00000	1.00000	1.000000
0.2	----	---	1.06801	1.06874	1.068750
0.4	---	---	1.13469	1.13521	1.135211
0.6	---	---	1.19912	1.19930	1.199300
0.8	1.261512	1.261479	1.26104	1.26099	1.261042
1.2	1.378052	1.377859	1.37772	1.37755	1.377554
2.0	----	----	1.58737	1.58740	1.587392

The Comparison Presented In Table 2, It Reveals That For The Selected Values Of The Parameters, The Values Of $-f''(0)$ Determined In This Study Are In Excellent Agreement With Some Previously Published Works.

5.0 Concluding Remarks

Heat Together With Mass Transport Of An Electrically Conducting Mhd Williamson And Casson Nano Fluid Model Have Been Solved Numerically Using Runge-Kutta Fehlberg Method Together With Shooting Technique. The Key Findings Of The Present Analysis Are As Follows:

(i) The Velocity Field Is A Degenerating Function Of β, M, We, A And S While The Velocity Field Elevate Due To Increase In The Value Of K;

(ii) The Temperature Field Is A Degenerating Function Of $\Pr$ And A While R Increases The Temperature Field;

(iii) The Concentration Field Is A Degenerating Function Of Sc, Kr, Nb And A While Nt Gives An Opposite Result; And

(iv) The Simultaneous Flow Of Casson And Williamson Nano Fluid Greatly The Rate Of Heat And Mass Transport.

References

[1] M. A.A. Mahmoud, S. E. Waheed, Mhd Flow And Heat Transfer Of A Micropolar Fluid Over A Stretching Surface With Heat Generation (Absorption) And Slip Velocity, Journal Of The Egyptian Mathematical Society (2012) 20, 20–27.
[2] S. Nadeem, S. T. Hussain And Changhoon Lee, Flow Of A Williamson Fluid Over A Stretching Sheet, Brazilian Journal Of Chemical Engineering, 30(3), (2013), 619 – 625.
[3] S. Bilal, Khalil Ur Rehman, M.Y. Malik. Numerical Investigation Of Thermally Stratified Williamson Fluid Flow Over A Cylindrical Surface Via Keller Box Method, Results In Physics 7 (2017) 690–696.
[4] N.T. Eldabe, M.Y. Abou-Zeid, Homotopy Perturbation Method For Mhd Pulsatile Non-Newtonian Nanofluid Flow With Heat Transfer Through A Non-Darcy Porous Medium, Journal Of The Egyptian Mathematical Society 25 (2017) 375–381.
[5] M. Bilal, M. Sagheer, S. Hussain, Numerical Study Of Magnetohydrodynamics And Thermal Radiation On Williamson Nanofluid Flow Over A Stretching Cylinder With Variable Thermal Conductivity, Alexandria Engineering Journal, 57, (2018), 3281–3289.
[6] Mair Khan, M.Y. Malik, T. Salahuddin, Arif. Hussian, Heat And Mass Transfer Of Williamson Nanofluid Flow Yield By An Inclined Lorentz Force Over A Nonlinear Stretching Sheet, Results In Physics 8 (2018) 862–868
[7] A. S. Idowu And B. O. Falodun, Soret–Dufour Effects On Mhd Heat And Mass Transfer Of Walter's-B Viscoelastic Fluid Over A Semi-Infinite Vertical Plate: Spectral Relaxation Analysis, Journal Of Taibah University For Science, 13:1, (2019), 49-62, Doi:10.1080/16583655.2018.1523527
[8]L. A. Lund, Zurni Omar, Ilyas Khan. Analysis Of Dual Solution For Mhd Flow Of Williamson Fluid With Slippage. Heliyon 5 (2019) E01345. Doi: 10.1016/J.Heliyon.2019. E01345.
[9] Hashim, Aamir Hamid, Masood Khan, Heat And Mass Transport Phenomena Of Nanoparticles On Time-Dependent Flow Of Williamson Fluid Towards Heated Surface, Neural Computing And Applications, (2019), 1-11 Https://Doi.Org/10.1007/S00521-019-04100-4(0123456789().
[10]A. M. Megahed, Williamson Fluid Flow Due To A Nonlinearly Stretching Sheet With Viscous Dissipation And Thermal Radiation, Journal Of The Egyptian Mathematical Society (2019) 27:12 , 1-10, Https://Doi.Org/10.1186/S42787-019-0016-Y
[11] Naganthran Kohilavani, Md Faisal Md Basir, Mohd Shareduwan Mohd Kasihmuddin, Sameh E. Ahmed, Falodun Bidemi Olumide, Roslinda Nazar, Exploration Of Dilatant Nanofluid Effects Conveying Microorganism Utilizing Scaling Group Analysis: Fdm Blottner, Physica A 549 (2020) 124040, 1-14.
[12] P. B. A. Reddy, Magnetohydrodynamic Flow Of A Casson Fluid Over An Exponentially Inclined Permeable Stretching Surface With Thermal Radiation And Chemical Reaction, Ain Shams Engineering Journal (2016) 7, 593–602.
[13] I. Ullah, Ilyas Khan, Sharidan Shafie, Hydromagnetic Falkner-Skan Flow Of Casson Fluid Past A Moving Wedge With Heat Transfer, Alexandria Engineering Journal (2016) 55, 2139–2148.
[14] S.S. Ghadikolaei, Kh. Hosseinzadeh, D.D. Ganjib, B. Jafari, Nonlinear Thermal Radiation Effect On Magneto Casson Nanofluid Flow With Joule Heating Effect Over An Inclined Porous Stretching Sheet, Case Studies In Thermal Engineering 12 (2018) 176–187
[15] A.I. Fagbade, B.O. Falodun, A.J. Omowaye, Mhd Natural Convection Flow Of Viscoelastic Fluid Over An Accelerating Permeable Surface With Thermal Radiation And Heat Source Or Sink: Spectral Homotopy Analysis Approach, Ain Shams Engineering Journal (2018) 9, 1029–1041.
[16] Falodun B.O., Onwubuoya C., And Awoniran Alamu F.H, Magnetohydrodynamics (Mhd) Heat And Mass Transfer Of Casson Fluid Flow Past A Semi-Infinite Vertical Plate With Thermophoresis Effect: Spectral Relaxation Analysis, *Defect And Diffusion Forum, Vol. 389, Pp 18-35 Doi:10.4028/Www.Scientific.Net/Ddf.389.18.*
[17] A. S. Idowu And B. O. Falodun (2020) Effects Of Thermophoresis, Soret-Dufour On Heat And Mass Transfer Flow Of Magnetohydrodynamics Non-Newtonian Nanofluid Over An Inclined Plate, Arab Journal Of Basic And Applied Sciences, 27:1, 149-165, Doi: 10.1080/25765299.2020.1746017.
[18] K Vijaya, G. V. Ramana Reddy, Influence Of Critical Parameters Of Thermophorosis On Mhd Non-Darcy Flow Of A Casson Fluid Past A Permeable Stretching Sheet, Frontiers In Heat And Mass Transfer (Fhmt) 14.

[19] M. Kalteh, Investigating The Effect Of Various Nanoparticle And Base Liquid Types On The Nanofluids Heat And Fluid Flow In A Microchannel, Applied Mathematical Modelling 37 (2013) 8600–8609.

[20] A. Ahmed, S. Nadeem, Shape Effect Of Cu-Nanoparticles In Unsteady Flow Through Curved Artery With Catheterized Stenosis, Results In Physics 7 (2017) 677–689.

[21] M. Farooq, M. Javed, M. Ijaz Khan, Aisha Anjum, T. Hayat, Melting Heat Transfer And Double Stratification In Stagnation Flow Of Viscous Nanofluid, Results In Physics 7 (2017) 2296–2301.

[22]J. Bowers, Hui Cao, Geng Qiao, Qi Li, Gan Zhang, Ernesto Mura, Yulong Ding (2018), Flow And Heat Transfer Behaviour Of Nanofluids In Microchannels, Progress In Natural Science: Materials International 28 (2018) 225–234.

[23]I. Khan And A. M. Alqahtani, Mhd Nanofluids In A Permeable Channel With Porosity, Symmetry 2019, 11, 378; Doi:10.3390/Sym11030378.

[24] A. J. Chamkha, A. M. Aly, And M. A. Mansour, "Similarity Solution For Unsteady Heat And Mass Transfer From A Stretching Surface Embedded In A Porous Medium With Suction/Injection And Chemical Reaction Effects," *Chemical Engineering Communications*, Vol. 197, No. 6, Pp. 846–858, 2010.

[25] S. Mukhopadhyay And R. S. R. Gorla, "Unsteady Mhd Boundary Layer Flow Of An Upper Convected Maxwell Fluid Past A Stretching Sheet With First Order Constructive/Destructive*engineering*, Vol. 9, No. 2, Pp. 123–133, 2012.

[26]M. Khan And M. Azam, "Unsteady Heat And Mass Transfer Mechanisms In Mhd Carreau Nanofluid Flow," *Journal Of Molecular Liquids*, Vol. 225, Pp. 554–562, 2017.

[27] Tesfaye Kebede, Eshetu Haile , Gurju Awgichew, And Tadesse Walelign, Heat And Mass Transfer In Unsteady Boundary Layer Flow Of Williamson Nanofluids, Journal Of Applied Mathematics
Volume 2020, Article Id 1890972, Pp.1-13 Pages, Https://Doi.Org/10.1155/2020/1890972

[28] P. N. Santoshi, Gv Ramana Reddy, P Padma, Numerical Scrutinization Of Three Dimensional Casson-Carreau Nano Fluid Flow, Journal Of Applied And Computational Mechanics 6 (3), (2020) 531-542.

[29]S. Sharidan, T. Mahmood, And I. Pop, "Similarity Solutions For The Unsteady Boundary Layer Flow And Heat Transfer Due To A Stretching Sheet," *International Journal Of Applied Mechanics And Engineering*, Vol. 11, Pp. 647–654, 2006.

Nomenclature

A	Initial Stretching Rate	V_0	Constant Value Of Velocity
B_0	Magnetic Field Of Constant Strength	η	Dimensionless Similarity Variable
C_f	Local Skin Friction Coefficient	$F(\eta)$	Dimensionless Stream Function
Cp	Specific Heat	$\theta(\eta)$	Dimensionless Temperature
C	Concentration Of The Fluid	$\phi(\eta)$	Dimensionless Concentration
Cw	Stretching Sheet Concentration	K	Permeability Parameter
T	Temperature Of The Fluid	β	Casson Parameter
κ	Thermal Conductivity	R	Radiation Parameter
D_b	Brownian Diffusion Coefficient	Nb	Brownian Motion Parameter
D_t	Thermophoresis Diffusion Coefficient	Nt	Thermophoresis Parameter
S	Suction/Injection Parameter	Sc	Schmidt Number
Q_r	Radiative Heat Flux	Kr	Chemical Reaction Parameter

M	Magnetic Parameter
T_∞	Ambient Temperature
K	Mean Absorption Coefficient
Pr	Prandtl Number
Re_x	Local Reynolds Number
Sh	Sherwood Number
U	Velocity Along X-Direction
V	Velocity Along Y-Direction
X,Y	Coordinates Axes
We	Weissenberg Number
A	Unsteadiness Parameter
U_w	Surface Velocity
T_w	Surface Temperature
C_w	Surface Concentration
V_w	Mass Transmission At The Surface Of The Plate